Journal of Applied Polymer Science

Natural Weathering Studies of Biobased Thermoplastic Starch from Agricultural Waste/Polypropylene Blends

Ming-Meng Pang,[1,2] Meng-Yan Pun,[2] Zainal Arifin Mohd. Ishak[1,3]

[1]School of Materials and Mineral Resources Engineering, Engineering Campus, Universiti Sains Malaysia, 14300 Nibong Tebal, Penang, Malaysia

[2]Texchem Polymers Research Centre, No. 1465, Mukim 11, Lorong Perusahaan Maju 6, Prai Industrial Estate, Phase 4, 13600 Prai, Penang, Malaysia

[3]Cluster for Polymer Composites, Engineering and Technology Research Platform, Science and Engineering Research Centre, Universiti Sains Malaysia, 14300 Nibong Tebal, Penang, Malaysia

Correspondence to: Z. A. M. Ishak (E-mail: zarifin.ishak@gmail.com)

ABSTRACT: Thermoplastic starch (TPS) obtained from agricultural waste was blended with polypropylene (PP) for natural weathering studies. The agricultural waste material was obtained from seeds and tubers with a starch content of approximately 50%. Commercial-grade TPS and native tapioca-based TPS were also prepared for comparison. The biobased TPS/PP extruded sheets were exposed to natural weathering for six months and their deterioration in weight, tensile properties, thermal properties, and relative molecular weight were monitored. SEM micrographs revealed the formation of surface cracking and the presence of microorganisms. FTIR spectrum indicated an increase in the carbonyl index over time as a result of the formation of degradation products. TPS/PP blends made from agricultural waste showed a better resistance to natural weathering compared to the other high starch formulation. The higher starch content in the blend system encouraged the rapid degradation process due to the combined effect of UV radiation with oxidation, moisture, temperature, and microbial attack. © 2013 Wiley Periodicals, Inc. J. Appl. Polym. Sci. 129: 3237–3246, 2013

KEYWORDS: degradation; polyolefins; thermoplastics; biopolymers and renewable polymers

Received 14 November 2012; accepted 21 January 2013; published online 20 February 2013
DOI: 10.1002/app.39054

INTRODUCTION

Thermoplastic starch (TPS) is a sustainable biobased product, as starch is a renewable resource. The two main disadvantages TPS has compared to most plastics currently in use have poor mechanical properties and high water solubility. To overcome these drawbacks, one option is to blend the TPS with a polyolefin such as polypropylene (PP). A biobased product that can be partially or fully made from renewable resource.[1,2] The TPS/PP blends prepared here are considered to be biobased materials. The benefits of biobased materials include having a renewable raw material source (i.e., starch), reducing the dependence on petrochemical-based polymer and mitigating the global warming by reducing the introduction of fossil carbon into the atmosphere.

Natural weathering testing is of interest, as it assesses the durability of a polymeric material after being exposed to a combination of environmental factors, such as sunlight, temperature, and rainfall. Typical thermoplastics undergo a change in physical properties after being exposed to natural weathering, such as color fading, surface cracking and deterioration of mechanical properties.[3,4] Ratanakamnuan and Aht-Ong[5] studied the photodegradation of LDPE/banana starch films and reported that a higher starch content and greater porosity allowed the easy access of light and oxygen into the interior parts of the films and resulted in a decrease in tensile properties. The deterioration of the properties of a material after the weathering test restricts its use in outdoor applications. Strategies, such as the addition of a UV stabilizer and antioxidant, can be adopted to preserve the useful shelf life and durability of plastic products.[6]

Most of the studies on TPS reported the utilization of starch derived from food crops, such as potato, wheat, rice, and corn, but not from agricultural waste.[7–11] These types of starch sources are important staple foods for the human population, as they possess a high starch content of over 70%. As a result, the use of food crops as feedstock has led to an argument over food-feed competition.[12] To avoid that conflict, this study focuses on the utilization of agricultural waste that can be converted into TPS. Two types of starch-containing agricultural

wastes have been identified: agricultural waste seed (AWS) and agricultural waste tuber (AWT). Both AWS and AWT can be easily obtained in Malaysia and within the neighboring countries, including Thailand and Indonesia. The AWS and AWT, with lower starch content (~50%), were used for the preparation of biobased TPS/PP blends. The AWS/PP and AWT/PP compounds were later shaped into extruded sheets for natural weathering degradation studies. Native tapioca starch (NTS) and a commercially available biobased sample (CS) were also used for comparison. The challenge addressed by this study is that agricultural waste contains a lower starch content compared to a normal starch source, and it therefore may fail to attain the desired plasticity and degradability. The driving force behind the use of agricultural waste is its low material cost, renewable origin and environmental benefits, such as the resolution of the waste disposal issue. There is also limited literature available regarding the agricultural-waste-derived TPS/PP blends and their degradation behavior under natural weathering. Thus, one of the aims of this study is to investigate how different compositions of amylose and amylopectin in the starch-containing agricultural waste will influence the tensile and weathering properties of PP.

EXPERIMENTAL

Materials

PP was supplied by Texchem Material Sdn Bhd, Malaysia. The melt flow index (MFI) and density of PP were 3.16 g/10 min (190°C/2.16 kg) and 0.90 g/cm^3, respectively. Maleic anhydride-grafted-PP (MA-*g*-PP) compatibilizer was manufactured by Arkema, with a 0.8 wt % maleic anhydride content, a density of 0.91 g/cm^3 and a melting temperature of 161°C. AWS (average particle size of 6.5 μm) and AWT (average particle size of 27.7 μm) were obtained from Texchem Material Sdn Bhd and had starch contents of 43.2% and 50.4%, respectively. The remaining details of the waste products are as follows: moisture (8–14%), protein (2–19%), fat (1–8%) and fiber (1–14%). NTS, supplied by Fumakilla Malaysia Berhad, had an average particle size of 4.3 μm, a starch content of 85.4% and moisture level of 11%. The amylose/amylopectin ratios for AWS, AWT, and NTS were 1:99, 26:74, and 29:71, respectively. Glycerin-based plasticizer, purchased from Texchem Material Sdn Bhd, had a density of 1.01 g/cm^3, an acid value <3% and a moisture <0.2%. Commercial grade biobased compound CS, with a biobased content of 52% (~70 wt % starch) per ASTM D6866 was obtained from Texchem Material Sdn Bhd. The MFI and density were 7.82 g/10 min (190°C/2.16 kg) and 1.19 g/cm^3, respectively.

Sample Preparation

A compound of starch powder (AWS, AWT, or NTS), PP and plastiziser was prepared with a ratio of 4:4:2. MA-*g*-PP was added to the formulation, comprising 3% of the total weight of the formulation. The single-step compounding was prepared in a Berstoff model twin-screw extruder with a length: diameter (*L/D*) ratio of 54:1. The compounding was performed at temperatures in the 140–170°C range, and the screw speed was set at 200 rpm. Sheet extrusion was performed in a Berlyn model single-screw extruder with an L/D ratio of 31:1. The sheet extruder processing temperature range was 150–170°C, and the screw speed was 50 rpm. The chill rolls temperature range was 60–80°C with a speed of 1.0–1.2 rpm. Four types of sheets, i.e., AWS/PP, AWT/PP, NTS/PP, and CS, were extruded to a thickness of 0.7 ± 0.1 mm.

Natural Weathering

The outdoor weathering test was carried out according to ASTM D1435 at the USM Engineering campus (latitude 5° 08' N, longitude 100° 29' E) for a period of 6 months from January to June 2011. Dumbbell specimens were mounted to a weathering rack and adjusted to face the equator at an angle of 45°. Specimens were collected after 1, 2, 4, and 6 month periods for the weight loss measurement and tensile properties assessment. The weight loss percentage was calculated with the following eq. (1):

$$\text{Weight loss } (\%) = \frac{W_b - W_a}{W_b} \times 100 \quad (1)$$

W_a and W_b are weight after weathering and weight before weathering, respectively.

Climate data (humidity, total rainfall, temperature, and UV radiation) during this period were obtained from Malaysia Meteorological Department.

Scanning Electron Microscopy (SEM)

Field emission SEM (model LEO Supra 50 VP, Germany) was used to observe the morphology of the specimens. Specimens were sputter-coated with a thin layer of gold to avoid electrical charging during examination.

Tensile Test

The tensile properties were determined with an Instron model 3366 tester (Instron, USA) according to ASTM D638 at a crosshead speed of 50 mm/min. Dumbbell specimens were cut from the extruded sheets according to the machine direction (MD) and transverse direction (TD) and conditioned at 24 ± 1°C and 50 ± 5% relative humidity for 2 days before test. The average of five measurements for the tensile strength (TS), elongation at break (EB) and Young's modulus (YM) were collected from the stress–strain data.

Differential Scanning Calorimetry (DSC)

Samples of ~7 mg were sealed in an aluminum pan, and thermal analysis measurement was performed using a Perkin Elmer DSC 8000 (USA). The equipment was programmed to work at a temperature range between 30°C and 200°C at a heating rate of 10°C/min. The values of melting temperature (T_m) and heat of fusion (ΔH_m) were obtained from the second heating. The degree of crystallinity (χ_c) was calculated by comparing the experimental heat of fusion obtained for the tested sample, ΔH_m with reference to a sample of 100% crystalline PP (ΔH_f) with the equation below (2):

$$x_c(\%) = \frac{\Delta H_m}{\Delta H_f(1 - W_f)} \times 100 \quad (2)$$

where W_f is the weight fraction of the fillers used.[13] The heat of fusion for 100% crystalline PP was reported as 207 J/g.[14]

Fourier Transform Infrared Spectroscopy (FTIR)

The FTIR model Perkin Elmer Spectrum One (USA) was used to obtain qualitative and quantitative information about the functional groups and chemical characteristics of the weathered specimens. The FTIR spectrum was recorded with 36 scans at a resolution of 2 cm^{-1}. The equipment was set to operate in the range of 550–4000 cm^{-1}. The carbonyl index (CI) was calculated as the ratio of the intensity (or area) of the peak at 1720 cm^{-1} to the reference peak intensity (or area) at 2917 cm^{-1} (which is the characteristic vibration of stretching band of PP).[15] The peak at 1720 cm^{-1} corresponded to the absorption from the presence of a carbonyl group, which was the by-product of polymer degradation.

Plate-Plate Rheometer

A plate-plate rheometer (model Physica MCR301, Anton Paar Germany) was used to obtain the viscosity curve of the weathered specimens with testing conditions of 180°C and shear rates in the range of 0.1 to 100 s^{-1}. Test specimens were cut into 20 mm diameters. The specimen was trapped between the movable plate and the stationary flat disk of the rheometer, which was equipped with an electronically commutated synchronous motor allowing real controlled stress and controlled strain tests. At low shear rates, polymer melts show a Newtonian behavior with a constant viscosity. The viscosity in the Newtonian regime is called the zero shear viscosity, η_0.[16] The zero shear viscosity is directly proportional to the weight-average molecular weight, M of the polymer melt, as shown in the following eq. (3):[17,18]

$$\eta_0 = KM^{3.4} \tag{3}$$

The parameter K is a material constant, and in this work, the relative M_1/M_2, before and after weathering can be calculated by using the following formula (4):

$$\log\left(\frac{\eta_1}{\eta_2}\right) = 3.4\log\left(\frac{M_1}{M_2}\right) \tag{4}$$

where η_1 is zero shear viscosity before weathering and η_2 is zero shear viscosity after weathering.

RESULTS AND DISCUSSION

Weight Loss

The percentage weight loss of the studied materials after exposure to natural weathering for 1, 2, 4, and 6 months is shown in Table I. Overall, the specimens in the MD and TD directions displayed a similar weight loss trend. The weight loss values are almost the same (statistically insignificant) for the same specimen regardless of the MD or TD directions. The CS weathering data were only available for short exposure times (2 months in MD and 1 month in TD) as beyond this period, the weight measurement became impossible because the specimens became brittle and broke into smaller pieces when light pressure was applied, as shown in Figure 1. A similar observation was reported for the NTS/PP, with only 4 months of data available. In this work, only the agricultural waste based materials AWT/PP and AWS/PP managed to survive for the entire 6 month weathering test.

Table I. Natural Weathering Weight Loss for CS, AWS/PP, NTS/PP, and AWT/PP

Orientation	Duration (month)	Weight loss (%)			
		CS	NTS/PP	AWT/PP	AWS/PP
MD	1	0.37	0.24	1.32	2.45
	2	1.78	0.36	2.08	3.42
	4	NA	3.08	12.16	17.70
	6	NA	NA	17.44	22.80
TD	1	0.67	0.2	1.39	1.58
	2	NA	0.25	2.60	2.60
	4	NA	3.57	12.88	17.45
	6	NA	NA	16.53	23.49

Natural weathering involves multiple modes of degradation and weight loss is one of the measurements for the degradation process. Sunlight is a rich source of UV radiation and polymers (both PP and starch components) exposed to sunlight undergo a rapid photo-initiation process. The matrix (i.e., PP) is susceptible to photo-oxidation, which involves the abstraction of a hydrogen atom (preferably tertiary hydrogen) by free radicals generated from hydro-peroxides, which are present in PP as impurities.[4,19] These radicals propagate, forming further radicals and resulting in chain scission of the polymer, thereby leading to a decrease in molecular weight. Cleaved chains are most frequently terminated by carboxylic groups and other functionalities such as esters and ketones.[20] The weight loss occurred because the low molecular weight oxidation products (i.e., acetone, carbon monoxide, acetic acid) can migrate from the matrix to the surface and subsequently evaporate or be washed away by rain water.[21] The photo-oxidation mechanisms for PP have been reported extensively by previous researchers.[4,22,23]

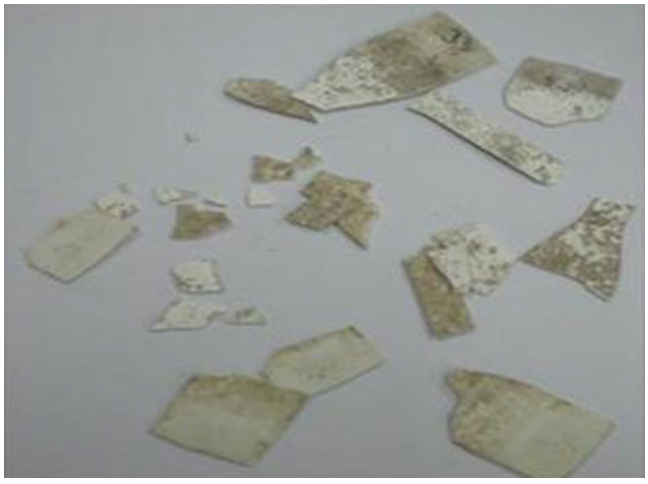

Figure 1. CS disintegrated after 2 months of weathering. [Color figure can be viewed in the online issue, which is available at wileyonlinelibrary.com.]

At the same time, starch can undergo photo-degradation with the formation of free radicals, resulting in the cleavage of the α (1–4) and α (1–6) bonds, shortening of the amylose chain and debranching of the amylopectin.[24,25] UV irradiation of starch granules can induce oxidative depolymerization and yield smaller molecules, e.g., dextrins, mono- and oligosaccharides.[26] Weight loss occurred after microorganisms consumed these simple sugars and smaller fragments of the polymer as their food source. The SEM images (Figures 2a-d) show the presence of microorganisms (i.e., *Chrysosporum* fungus) and crack lines on the specimen's surface. The development of the crack lines allowed more water to penetrate, which subsequently promoted the entrance of microorganisms to begin the biodegradation. In addition, the starch granules located at the outer surface may leach out after being washed away by rain water and contribute to the weight loss.

The weight loss reported for CS and NTS/PP before disintegration was approximately 0.7–3.6%. The rapid disintegration in CS and NTS/PP may be attributed to their higher starch content in the blends system. Starch added into the synthetic polymer (i.e., PP) created a porous structure that could enhance the accessibility of water, oxygen and microorganisms into the polymer matrix. The starch granules swelled after absorbing moisture and shrank during hot days; this cycle would again contributed to cracks on the exposed surface that could accelerate degradation.[27] AWS/PP showed 6% more weight loss than AWT/PP after 6 months of natural weathering. AWS contained amylopectin almost exclusively, with no amylose, while AWT contained 26% amylose. According to Ke et al.,[28] the water absorption of high amylopectin starch was higher than blends made with high-amylose starch. Thus, the higher water absorption of AWS/PP could encourage greater growth of microorganisms because of the higher water availability within the material; the starch is consumed by the microorganisms resulting in overall higher weight loss.

Tensile Properties

The tensile properties of the studied materials in the MD and TD directions are shown in Tables II and III, respectively. The humid tropical climate data during the weathering period is shown in Table IV. In general, the tensile performance (i.e., TS, EB) of the control specimen in the MD was significantly higher than the TD ($P < 0.05$). This is because the polymer chains are highly oriented in MD and strong covalent bonds are present between carbon atoms along the polymer chains, thereby giving greater strength in that direction. The lack of molecular alignment in the TD results in weak van der Waals bonds between polymer chains; thus, less energy is required to break the TD-oriented specimens.[29,30]

Overall, the specimens, regardless of MD or TD orientation, showed a decline in tensile strength (TS) after natural weathering. The TS loss % increased with an increase in exposure time. Both the MD- and TD-oriented specimens displayed a similar

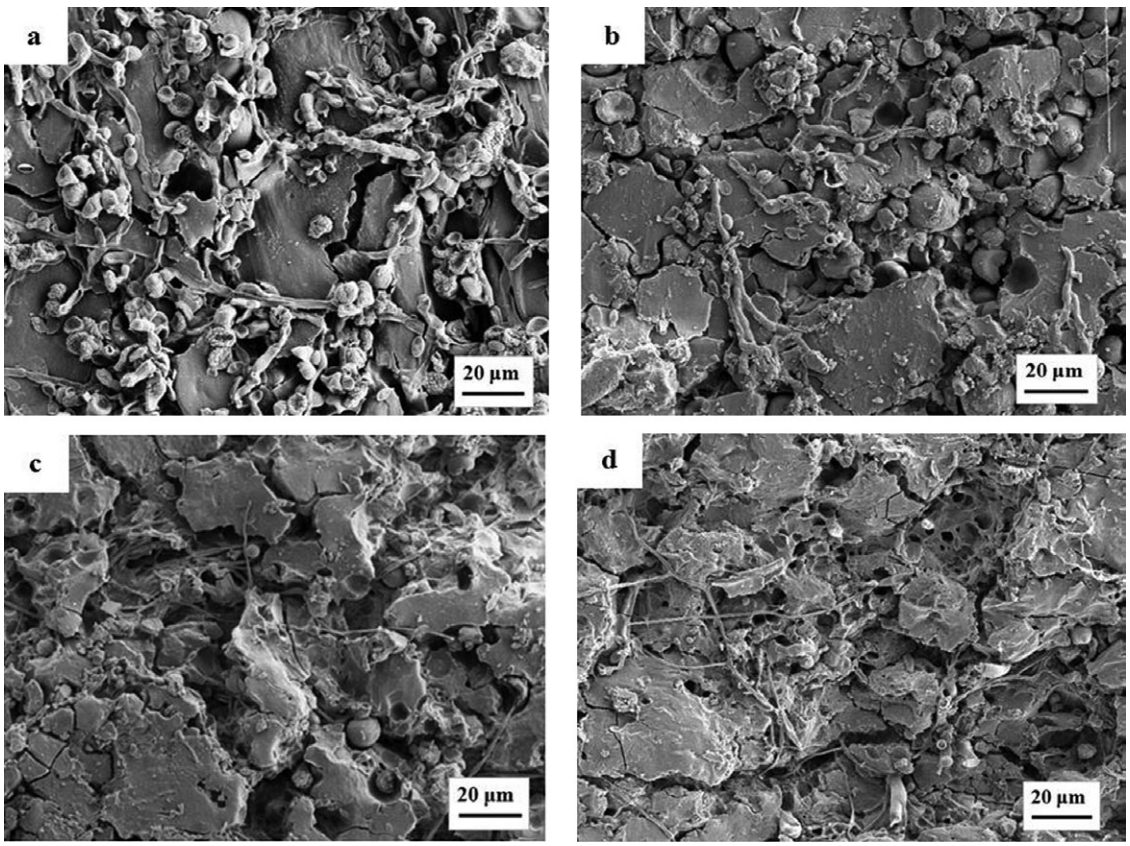

Figure 2. (a) SEM micrograph of 2 months weathered CS. (b) SEM micrograph of 4 months weathered NTS/PP. (c) SEM micrograph of 6 months weathered AWT/PP. (d) SEM micrograph of 6 months weathered AWS/PP.

Table II. Tensile Properties for CS, NTS/PP, AWT/PP, and AWS/PP (Machine Direction) Before and After Weathering

Weathering			CS	NTS/PP	AWT/PP	AWS/PP
MD	Zero	TS (MPa)	7.5 ± 0.9	16.0 ± 1.2	17.7 ± 1.9	19.9 ± 1.7
		EB (%)	15.7 ± 3.9	383 ± 36	76.6 ± 12.3	489 ± 35
		YM (MPa)	660 ± 19	535 ± 22	677 ± 27	547 ± 16
	1 month	TS (MPa)	2.1 ± 0.6	11.7 ± 0.8	18.0 ± 0.5	17.3 ± 0.5
			[−72.0]	[−26.9]	[+1.7]	[−13.1]
		EB (%)	0.8 ± 0.3	11.7 ± 4.1	19.2 ± 1.0	168 ± 24
			[−94.9]	[−96.9]	[−74.9]	[−65.6]
		YM (MPa)	316 ± 12	522 ± 28	440 ± 13	489 ± 18
			[−52.1]	[−2.4]	[−35.0]	[−10.6]
	2 months	TS (MPa)	0.9 ± 0.0	8.4 ± 1.7	10.3 ± 0.2	15.6 ± 1.0
			[−88.0]	[−47.5]	[−41.8]	[−21.6]
		EB (%)	0.3 ± 0.0	2.2 ± 0.5	4.3 ± 0.7	17.2 ± 5.0
			[−98.1]	[−99.4]	[−94.4]	[−96.5]
		YM (MPa)	272 ± 0	511 ± 14	439 ± 14	426 ± 19
			[−58.8]	[−4.5]	[−35.2]	[−22.1]
	4 months	TS (MPa)	NA	3.4 ± 0.4	8.2 ± 1.2	13.5 ± 1.5
				[−78.8]	[−53.7]	[−32.2]
		EB (%)	NA	1.9 ± 0.2	3.0 ± 0.3	4.7 ± 1.5
				[−99.5]	[−96.1]	[−99.0]
		YM (MPa)	NA	233 ± 10	450 ± 26	518 ± 27
				[−56.4]	[−33.5]	[−5.3]
	6 months	TS (MPa)	NA	NA	3.3 ± 1.1	9.7 ± 1.6
					[−81.4]	[−51.3]
		EB (%)	NA	NA	1.2 ± 0.1	2.6 ± 0.7
					[−98.4]	[−99.5]
		YM (MPa)	NA	NA	278 ± 76	511 ± 21
					[−58.9]	[−6.6]

TS loss [% indicated in square brackets]; in other words, the effect of weathering is the same for the MD- and TD-oriented specimens. For example, the AWT/PP after 6 months weathering experienced 81.4% loss for the MD and 83.1% loss for the TD. The different between these values is statistically insignificant. The deterioration in TS is in accordance with the results reported by Sam et al.[31] and Al-Shabanat[3] for polyolefin composites. In an outdoor environment, PP undergoes photo-oxidation after being exposed to UV radiation from sunlight, which causes changes in thermal behavior, initiates surface cracking and weakens mechanical properties.[32] Merlin and Fouassier[33] reported that UV irradiation of starch resulted in chain scission and radical generation on the glucosidic ring. The UV-induced depolymerization occurred in both amylopectin and amylose, while cross-linking occurred mainly in amylose fractions.[26] The degradation of starch synergistically enhanced the abiotic oxidative degradation reaction of the blend system.

Degradation happened rapidly during the early stage of the weathering test, particularly for CS (MD) where TS declined drastically, with a loss of up to 88% in only 2 months. The CS (TD) was even worse, with 76% TS loss in 1 month; afterwards, all specimens were fragmented rendering tensile measurement impossible. The CS with the highest starch content showed the greatest loss in TS. The incorporation of starch into the synthetic polymer makes the blend system more susceptible to degradation. This finding is supported by the work of Erlandsson et al.[34] The authors reported that in the UV-exposed samples, LDPE-starch is more degradable than pure LDPE, indicating that in a photo-degrading environment, starch has a positive effect on degradation rate. The NTS (starch content >85%) blended with PP ranked second in the weathering test for rapid degradation, and the tensile test could only be carried out to 4 months of exposure. The AWS and AWT with low-starch (43% and 50%, respectively) blends survived the full term of 6 months of natural weathering, but they experienced a TS loss of over 50%. Starch's exposure to a radiation source leads to oxidative depolymerization, predominantly in the less-organized amorphous zone.[26,35] In this study, it was observed that material rich in amylose is more susceptible to UV-degradation; NTS/PP contained the highest ratio of amylose, followed by AWT/PP and AWS/PP. This finding may also explain the sharp drop in the tensile properties of the NTS/PP over the AWT/PP and AWS/PP. The AWS/PP, which had almost no amylose content,

Table III. Tensile Properties for CS, NTS/PP, AWT/PP, and AWS/PP (Transverse Direction) Before and After Weathering

Weathering			CS	NTS/PP	AWT/PP	AWS/PP
TD	Zero	TS (MPa)	5.3 ± 0.7	13.5 ± 1.1	13.6 ± 0.7	15.6 ± 2.3
		EB (%)	5.9 ± 1.6	344 ± 32	10.5 ± 1.1	371 ± 47
		YM (MPa)	547 ± 15	563 ± 10	622 ± 22	456 ± 36
	1 month	TS (MPa)	1.3 ± 0.0	9.5 ± 0.1	10.2 ± 0.8	9.8 ± 0.9
			[−75.5]	[−29.6]	[−25.0]	[−37.2]
		EB (%)	0.7 ± 0.0	3.7 ± 1.2	7.1 ± 1.6	43.2 ± 8.4
			[−88.1]	[−98.9]	[−32.4]	[−88.4]
		YM (MPa)	190 ± 4	524 ± 6	413 ± 28	413 ± 21
			[−65.3]	[−6.9]	[−33.6]	[−9.4]
	2 months	TS (MPa)	NA	6.7 ± 0.3	7.9 ± 0.2	12.7 ± 0.9
				[−50.4]	[−41.9]	[−18.6]
		EB (%)	NA	1.3 ± 0.0	3.6 ± 1.0	5.8 ± 1.1
				[−99.6]	[−65.7]	[−98.4]
		YM (MPa)	NA	509 ± 20	410 ± 38	381 ± 8
				[−9.6]	[−34.1]	[−16.4]
	4 months	TS (MPa)	NA	3.1 ± 0.3	5.9 ± 0.3	8.5 ± 1.4
				[−77.0]	[−56.6]	[−45.5]
		EB (%)	NA	1.5 ± 0.2	2.4 ± 0.4	3.2 ± 1.0
				[−99.6]	[−77.1]	[−99.1]
		YM (MPa)	NA	241 ± 22	319 ± 18	406 ± 37
				[−57.2]	[−48.7]	[−11.0]
	6 months	TS (MPa)	NA	NA	2.3 ± 0.9	6.0 ± 0.7
					[−83.1]	[−61.5]
		EB (%)	NA	NA	0.9 ± 0.2	1.8 ± 0.2
					[−91.4]	[−99.5]
		YM (MPa)	NA	NA	271 ± 59	404 ± 16
					[−56.4]	[−11.4]

showed the least deterioration of TS, with 51.3–61.5% loss, compared to the AWT/PP, with 81.4–83.1% loss after 6 months of weathering. This finding is in agreement with a previous study by Vatanasuchart et al.[36] The authors reported the amylose embedded in the amorphous background regions were more likely to be degraded by UV radiation than the amylopectin, based on the shift of the molecular weight distribution. A previous study by Sandhu et al.[37] also reported that the linear structure and random arrangement of amylose makes it more susceptible to oxidative degradation.

In addition to the deterioration in TS, all specimens, regardless of orientation, also encountered a drastic decline in elongation at break (EB). There was no significant difference in the EB loss % encountered by the same specimen with different orientations. The CS and NTS/PP recorded a rapid degradation in EB in a short exposure period, i.e., more than 90% EB loss in the first month. Even the AWS/PP and AWT/PP, after 6 months of weathering showed a similarly high EB loss of over 90%. The deterioration in EB is in agreement with the result reported by Sam et al.,[31] not only was TS affected, but EB also decreased

Table IV. Penang Climate Data from January to June 2011

Month	UV radiation (J/m^2)	Max. temp. (°C)	Min. temp. (°C)	Avg. temp. (°C)	Max. humidity (%)	Min. humidity (%)	Avg. humidity (%)	Total rainfall (mm)
Jan	2598.1	28.3	24.9	27.0	93.1	59.8	76.9	76.6
Feb	3593.3	28.9	26.7	28.0	82.5	66.0	75.5	33.2
March	3877.3	28.9	25.1	27.0	94.6	72.4	84.7	402.6
April	3749.5	29.3	25.8	28.1	93.0	70.0	81.2	232.0
May	3641.6	29.9	25.7	28.3	94.5	76.8	82.4	161.6
June	3217.4	29.4	26.3	28.4	88.8	74.0	80.1	54.2

after exposure to natural weathering. The specimen's surface crack, as displayed in the earlier SEM micrograph, is one of the main reasons for the reduction in EB. According to Yoshii et al.,[38] EB is a very useful indicator of polymer degradation. In this work, deterioration in EB is clear and even more sensitive than TS as an indicator of natural weathering degradation of the polymer material. The other possible cause for the dramatic reduction in the EB is the loss of plasticizer. Plasticizer can directly evaporate from the surface of the specimen or diffuse through the polymer matrix up to the surface and be lost to the surrounding medium, most often the air.[39] The development of crack lines on the surface exposes the inner layer to atmospheric factors (i.e., heat, light, and rain), which accelerates the loss of plasticizer through migration and evaporation.[40,41] The primary role of plasticizer is to improve the flexibility and distensibility of polymer chains. Once the plasticizer content is reduced or lost, the specimen loses its flexibility and cannot elongate to the extent it previously could.

Young's modulus (YM) for weathered specimens can be seen in Tables II and III. As discussed earlier, the weathering effect is the same for same specimen regardless of the MD or TD, and this fact also applies to the YM loss. All specimens encountered modulus losses over 50% by the end of the weathering test, except the AWS/PP, which had a loss of 6–11%. The retention in YM of the AWS/PP may be attributed to its high amylopectin content, which is less susceptible to photodegradation compared with the NTS/PP and AWT/PP. In addition, the minimum YM loss in the AWS/PP could be related to the small reduction in the crystallinity after weathering, as shown in Table V (discussed in the next section), whereby the AWT/PP and NTS/PP showed a higher loss in crystallinity and subsequently a greater loss in modulus. A previous study by Van der Wal et al.[42] showed that the tensile modulus of the PP increased with the increase in crystallinity. The overall reduction in YM and other tensile properties (i.e., TS, EB) is due to the combined effect of chain scission in PP, depolymerization of starch, reduced starch-matrix interfacial bonding and the formation of surface cracks. Beg and Pickering[43] reported similar findings, in which PP wood composites after weathering showed a reduction in TS and YM. However, several authors[3,31,44] reported that YM increased after weathering related to increases in crystallinity and rearrangement of molecules processes that increased embrittlement. If the specimen is exposed to natural weathering for a longer period, it will develop increasingly severe surface cracks while simultaneously allowing other degradation processes to take place (e.g., chemical degradation, water absorption, microorganisms attack) that could eventually deteriorate the properties of the specimen.[32]

Table V. DSC Data for CS, NTS/PP, AWS/PP, and AWT/PP Before and After Weathering

	T_m (°C)		ΔH_m (J/g)		χ_c (%)	
Sample	Before	After	Before	After	Before	After
CS	160.5	153.0	34.3	20.0	NA	NA
NTS/PP	161.6	153.7	36.6	27.0	35.4	26.1
AWS/PP	157.3	156.7	27.9	26.7	27.0	25.8
AWT/PP	159.6	157.2	29.1	21.9	28.1	21.2

DSC Results

The DSC curves (second heating step) for all studied materials are shown in Figure 3. The DSC data, i.e., melting peak temperature (T_m), heat of fusion (ΔH_m) and degree of crystallinity (χ_c) for the CS obtained after 2 months, NTS/PP after 4 months, AWS/PP and AWT/PP after 6 months of weathering are shown in Table V. The χ_c for the CS cannot be determined, as the polyolefin composition is undisclosed. Overall, specimens showed a decline in the T_m and ΔH_m, which led to a drop in the χ_c (1.2–9.3% lower). In this work, AWS/PP experienced minimum changes in melting temperature and crystallinity after weathering; thus, this compound can maintain most of its tensile properties (i.e., TS and YM) compared to other PP/starch blends. The reduction in T_m and χ_c for weathered PP composites is supported by previous studies.[32,43] In contrast, some researchers reported an increment in crystallinity for PP based weathered specimens.[45,46] The changes in crystallinity of weathered specimens could be related to exposure conditions. PP contains impurities (catalyst residues) that are present during the manufacturing, which make it sensitive to UV radiation.[47] The impurities are capable of absorbing the radiation energy and act as a catalyst for photodecomposition. Because the PP crystalline regions are impermeable to oxygen, degradation can occur predominantly in the amorphous regions by chain scission. The chain scission allows the smaller molecules to rearrange, and it results in an increase in the degree of crystallinity.[48] However, as chain scissions continue to occur, they can affect the tie molecules (chain traversing the amorphous phase from one crystalline lamella to another) and result in the degradation of crystallinity and the appearance of surface cracks.[49] In the case of UV-irradiated LDPE/thermoplastic pea starch, Raquez et al.[24] reported that the crystallinity of the LDPE matrix increased for the first 11 weeks due to the re-crystallization of smaller segments. Once the UV-irradiation time exceeded 13 weeks, degradation occurred through the main polyolefin backbone and led

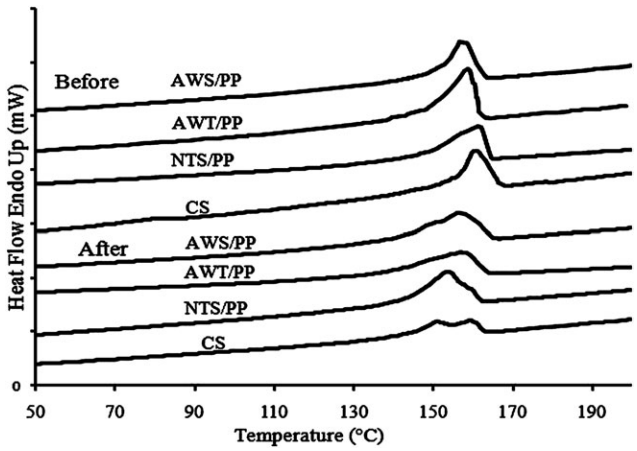

Figure 3. DSC curves for CS, NTS/PP, AWT/PP, and AWS/PP before and after weathering.

Applied Polymer SCIENCE

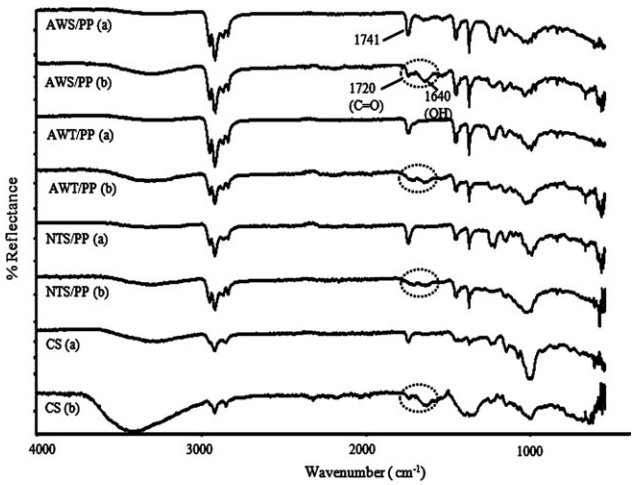

Figure 4. FTIR spectrums (a) before weathering and (b) after weathering for CS, NTS/PP, AWT/PP, and AWS/PP.

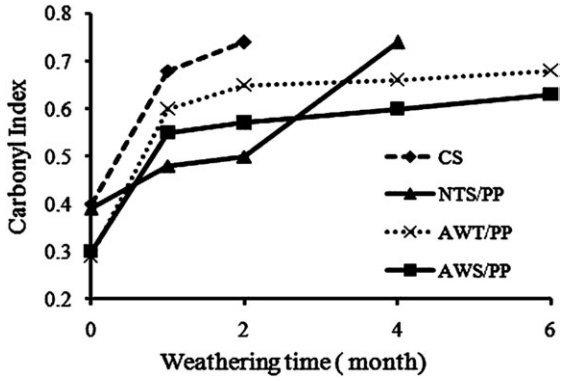

Figure 5. Carbonyl index for CS, NTS/PP, AWT/PP, and AWS/PP over weathering time.

to a decrease in the degree of crystallinity. Thus, the reduction of the crystallinity in this study could be attributed to the more advanced stage of degradation. The PP, after exposure to weathering for a long time, changed from ductile to brittle. In addition, the generation of photodegradation products such as carbonyls which are attached to the molecular segments decreased the close-packing ability that hinders crystallization.[32]

FTIR Results

The FTIR spectrum can be used to study the changes that occurred in the weathered specimens, especially the presence of degradation products, such as carboxylic and carbonyl groups (in a wide range of 1665–1760 cm^{-1}).[3,50,51] CS weathered after 2 months, NTS/PP weatherd after 4 months, AWS/PP, and AWT/PP weathered after 6 months were used in the FTIR analysis. The FTIR spectra for before and after weathering are shown in Figure 4. Referring to spectrum (a) for the AWS/PP, AWT/PP, and NTS/PP, all specimens showed an absorption peak at 1741–1745 cm^{-1}, which was assigned to the plasticizer that consisted of an ester group. A similar peak was observed in CS, which means it may include ester as part of the formulation. The characteristic bands for starch include wave numbers 3000–3650 cm^{-1} (O—H stretching), 2926 cm^{-1} (C—H stretching), 1640 cm^{-1} (O—H bending), 1461 cm^{-1} (CH_2 bending), 1445–1325 cm^{-1} (C—H bending and wagging) and 1244–1022 cm^{-1} (C—O stretching). The characteristic bands for PP include the 2952–2830 cm^{-1} (C—H stretching), 1456 cm^{-1} and 1376 cm^{-1} for asymmetry and symmetry bending C—H (—CH_3) and 1165 cm^{-1} (bending vibration of tertiary carbon).[3,50,52]

Significant changes in the hydroxyl (O—H) and carbonyl (C=O) regions were observed after weathering. As shown in spectrum (b), all weathered specimens showed a strong O—H band in the region of 1630–1646 cm^{-1}. An increase in the O—H stretching band at 3200–3600 cm^{-1} was also observed. The broad 1640 cm^{-1} O—H band can be attributed to the water molecules absorbed by the starch molecules.[52,53] This intense O—H peak is caused by the high water absorption of the weathered specimens from the environment.[54] FTIR-ATR is a surface analysis method and the specimen's surface absorbed the most moisture.

Many researchers have used the carbonyl index as a parameter to observe surface oxidation and degradation of the blends system.[15,34,55] In this work, the carbonyl group region was located at a higher wave number than the hydroxyl region of 1640 cm^{-1}. The carbonyl index was quantified from the intensity wave number of 1665 to 1720 cm^{-1} with reference peak at 2917 cm^{-1} (C—H stretching). Figure 5 shows the carbonyl index of the weathered specimens over time. This index showed a gradual increase (i.e., more degradation products were generated) with the increase in weathering time, which is in accordance with findings reported by previous researchers.[15,45,56]

Viscosity Result

Specimens after exposure to natural weathering, experienced multimodes of degradation, including chain scission during photo-oxidation. Thus, the reduction in molecular weight is one of the measurements of the degradation process. In this work, a plate-plate rheometer was used to study molecular

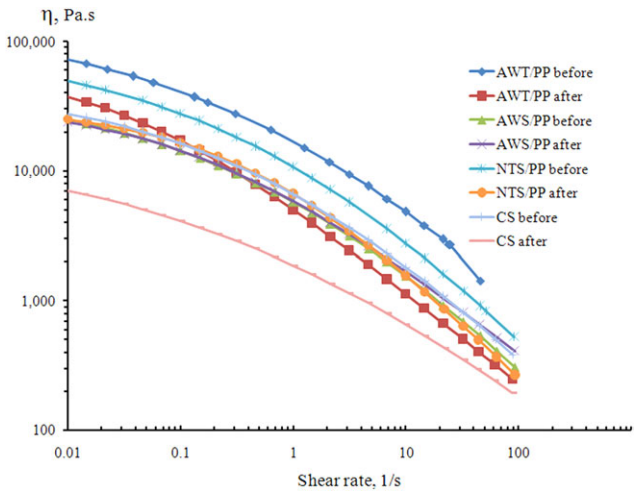

Figure 6. Viscosity curves for CS, NTS/PP, AWS/PP, and AWT/PP before and after weathering. [Color figure can be viewed in the online issue, which is available at wileyonlinelibrary.com.]

Table VI. The Relative Molecular Weight (M_1/M_2), Before and After Weathering for CS, NTS/PP, AWT/PP, and AWS/PP

Sample	Zero shear viscosity (Pa s)		η_1/η_2	M_1/M_2
	Before (η_1)	After (η_2)		
CS	47,300	15,600	3.03	1.39
NTS/PP	94,400	31,500	3.00	1.38
AWT/PP	161,000	66,000	2.44	1.30
AWS/PP	47,900	35,700	1.34	1.09

weight changes for weathered specimen through shear viscosity extrapolation at a low shear rate.

Figure 6 shows the diagram of the viscosity versus shear rate for studied materials before and after being subjected to natural weathering. The zero shear viscosity was taken from the extrapolation of the graph at the low shear rate and represents the weight-average molecular weight of the specimen.[57] Table VI shows the values of relative molecular weight, M_1/M_2, for the studied materials before and after weathering. CS showed the highest M_1/M_2 value, which means that the molecular weight of the weathered specimen was drastically reduced; the molecular weight before weathering was 1.39 times higher than after weathering. This result may explain the sharp reduction in tensile properties for CS, as it degraded faster and experienced the highest molecular weight change among all of the specimens. All of the specimens showed a reduction in the molecular weight after weathering. The molecular weight changes, M_1/M_2, in descending order were CS>NTS/PP>AWT/PP>AWS/PP. NTS/PP ranked second after CS, as it also showed a relatively high M_1/M_2 of 1.38. This result agrees with the earlier discussion regarding the fact that NTS/PP tensile data are only available for up to 4 months while AWT/PP and AWS/PP survived for the full term of 6 months of natural weathering. AWT/PP showed a higher reduction in molecular weight than AWS/PP. This result is in accordance with previous discussions, where AWT/PP degraded faster than AWS/PP with a higher carbonyl index.

CONCLUSIONS

This work examined the degradation of biobased materials after exposure to natural outdoor weathering. Weathered specimens experienced weight loss and a reduction in tensile properties (TS, EB and YM). Additionally, it was reported that the materials rich in amylose were more susceptible to photodegradation than those containing high amylopectin starch. SEM studies showed the growth of surface cracks and the appearance of colonies of microorganisms. The carbonyl index also increased over exposure time, indicating the presence of degradation products. The zero shear viscosity, which represents the molecular weight of the specimens, decreased after natural weathering. The TPS/PP blends made from agricultural waste, i.e., AWS and AWT, showed better resistance to natural weathering compared to the high starch formulations (CS and NTS/PP). The low starch content in the agricultural waste reduced the occurrence of the starch swelling-shrinkage cycles; thus, it slowed the crack propagation and decreased the risk of microbial attack. In contrast, the high starch content in CS and NTS/PP encouraged rapid degradation process as more starch granules led to a porous structure and increased the penetration of water, light, oxygen, and microbial attack.

ACKNOWLEDGMENTS

The financial support from Texchem Polymers Sdn Bhd is greatly appreciated. Technical and equipment support from the School of Materials and Mineral Resources Engineering, USM is also acknowledged.

REFERENCES

1. Jong, E. D.; Higson, A.; Walsh, P.; Wellisch, M. Task 42 Biobased Chemicals. Available at: http://www.ieabioenergy.com/LibItem.aspx?id=7311 (accessed 17 Oct 2012).
2. PlasticsEurope. PlasticsEurope's view on "bioplastics". Available at: http://www.plasticseurope.org/documents/document/20120522112447-plastics_industry_view_on_bioplastics_v16052012.pdf (accessed 17 Oct 2012).
3. Al-Shabanat, M. *IJC* **2011**, *3*, 129.
4. Rajakumar, K.; Sarasvathy, V.; Chelvan, A.T.; Chitra, R.; Vijayakumar, C. T. *J. Polym. Environ.* **2009**, *17*, 191.
5. Ratanakamnuan, U.; Aht-Ong, D. *J. Appl. Polym. Sci.* **2006**, *100*, 2725.
6. Zeus. Weathering of Plastics. Available at: http://www.zeusinc.com/UserFiles/zeusinc/Documents/Zeus_Weathering_of_Plastics.pdf (accessed November 2011).
7. Bikiaris, D.; Pavlidou, E.; Prinos, J.; Aburto, J.; Alric, I.; Borredon, E.; Panayiotou, C. *Polym. Degrad. Stab.* **1998**, *60*, 437.
8. Li, G.; Sarazin, P.; Orts, W. J.; Imam, S. H.; Favis, B. D. *Macromol. Chem. Phys.* **2011**, *212*, 1147.
9. Prachayawarakorn, J.; Sangnitideh, P.; Boonpasith, P. *Carbohydr. Polym.* **2010**, *81*, 425.
10. Sabetzadeh, M.; Bagheri, R.; Masoomi, M. *J. Appl. Polym. Sci.* **2012**, *126*, 63.
11. Swinkels, J. J. M. Starch/Stärke **1985**, *37*, 1.
12. Kim, S.; Dale, B. E. *Biomass Bioenergy* **2004**, *26*, 361.
13. Lee, T. H.; Boey, F. Y. C.; Khor, K. A. *Compos. Sci. Technol.* **1995**, *53*, 259.
14. Ehrenstein, G. W.; Riedel, G.; Trawiel, P. Thermal Analysis of Plastics; Hanser: Munich, **2004**, p 14.
15. La Mantia, F. P.; Morreale, M. *Polym. Degrad. Stab.* **2008**, *93*, 1252.
16. Lauger, J.; Bernzen, M. *Annual Transact. Nordic Rheol. Soc.* **2000**, *8*, 159.
17. White, J. L. Principles of Polymer Engineering Rheology; Wiley: United States, **1990**, p 139.
18. Nichetti, D.; Manas-Zloczower, I. *J. Rheol.* **1998**, *42*, 951.
19. Carlsson, D. J.; Lacoste, J. *Polym. Degrad. Stab.* **1991**, *32*, 377.
20. Arkatkar, A.; Arutchelvi, J.; Sudhakar, M.; Bhaduri, S.; Uppara, P.V.; Doble, M. *Open Environ. Eng. J.* **2009**, *2*, 68.

21. Czegeny, Z. S.; Jakab, E.; Vig, A.; Zelei, B.; Blazso, M. J. *Anal. Appl. Pyrolysis* **2000**, *56*, 229.
22. Singh, B.; Sharma, N. *Polym. Degrad. Stab.* **2008**, *93*, 561.
23. Rivaton, A.; Serre, F.; Gardette, J. L. *Polym. Degrad. Stab.* **1998**, *62*, 127.
24. Raquez, J.-M.; Bourgeois, A.; Jacobs, H.; Degee, P.; Alexandre, M.; Dubois, P. *J. Appl. Polym. Sci.* **2011**, *122*, 489.
25. Bhat, R.; Karim, A. A. *Compr. Rev. Food Sci. Food Saf.* **2009**, *8*, 44.
26. Fiedorowicz, M.; Tomasik, P.; You, S.; Lim, S-T. *Starch/Stärke* **1999**, *51*, 126.
27. Yew, G. H.; Mohd Yusof, A. M.; Mohd Ishak, Z. A.; Ishiaku, U. S. Natural weathering effects on the mechanical properties of polylactic acid/rice starch composites, Proceeding of the 8th Polymers for Advanced Technologies International Symposium, Hungary, **2005**; p 1–3.
28. Ke, T.; Sun, S. X.; Seib. P. *Appl. Polym. Sci.* **2003**, *89*, 13, 3639.
29. Bower, D. I. An Introduction to Polymer Physics; Cambridge University Press: UK, **2002**, p 383.
30. Kubisiak, M. P.; Quesnel, D. J. *Polym. Eng. Sci.* **1996**, *36*, 17, 2253.
31. Sam, S. T.; Ismail, H.; Ahmad, Z. *Polym.-Plast. Technol. Eng.* **2011**, *50*, 957.
32. Leong, Y. W.; Abu Bakar, M. B.; Mohd Ishak, Z. A.; Ariffin, A. *Polym. Degrad. Stab.* **2004**, *83*, 411.
33. Merlin, A.; Fouassier, J.-P. *Macromol. Chem. Phys.* **1981**, *182*, 11, *3053*-3068.
34. Erlandsson, B.; Karlsson, S.; Albertsson, A. C. *Polym. Degrad. Stab.* **1997**, *55*, 237.
35. Ciesla, K. J. *Therm. Anal. Calorim.* **2003**, *74*, 259.
36. Vatanasuchart, N.; Naivikul, O.; Charoenrein, S.; Sriroth, K. *Carbohydr. Polym.* **2005**, *61*, 80.
37. Sandhu, K. S.; Kaur, M.; Singh, N.; Lim, S.-T. L. W.T. *Food Sci. Technol.* **2008**, *41*, 1000.
38. Yoshii, F.; Meligi, G.; Sasaki, T.; Makuuchi, K.; Rabie, A. M.; Nishimoto, S. *Polym. Degrad. Stab.* **1995**, *49*, 315.
39. Kovacic, T.; Mrklic, Z. *Thermochim. Acta* **2002**, *381*, 49.
40. Vieira, M. G. A.; Silva, M. A. D.; Santos, L. O. D.; Beppu, M. M. *Eur. Polym. J.* **2011**, *47*, 254.
41. Rosato, D. V. Rosato's Plastics Encyclopedia and Dictionary; Hanser Publisher: Munich, **1993**, p 539.
42. Van der Wal, A.; Mulder, J. J.; Gaymans, R. J. *Polymer* **1998**, *39*, 22, 5477.
43. Beg, M. D. H.; Pickering, K. L. *Polym. Degrad. Stab.* **2008**, *93*, 1939.
44. Mendes, L. C.; Rufino, E. S.; Paula, F. O. C. D.; Torres A. C. Jr. *Polym. Degrad. Stab.* **2003**, *79*, 371.
45. Li, J.; Yang, R.; Yu, J.; Liu, Y. *Polym. Degrad. Stab.* **2008**, *93*, 84.
46. Craig, I. H.; White, J. R.; Phua, C. H. *Polymer* **2005**, *46*, 505.
47. Lucas, N.; Bienaime, C.; Belloy, C.; Queneudec, M.; Silvestre, F.; Nava-Saucedo, J. E. Chemosphere **2008**, *73*, 4, 429.
48. Yakimets, I.; Lai, D; Guigon, M. *Polym. Degrad. Stab.* **2004**, *86*, 59.
49. Stark, N. M.; Matuana, L. M. *J. Appl. Polym. Sci.* **2004**, *94*, 2263.
50. Kaczmarek, H.; Oldak, D.; Malanowski, P.; Chaberska, H. *Polym. Degrad. Stab.* **2005**, *88*, 189.
51. Oliani, W. L.; Parra, D. F.; Lugao, A. B. *Radiat. Phys. Chem.* **2010**, *79*, 383.
52. Chandra, R.; Rustgi, R. *Polym. Polym. Degrad. Stab.* **1997**, *56*, 185.
53. Zhang, S. D.; Zhang, Y. R.; Zhu, J.; Wang, X. L.; Yang, K. K.; Wang, Y. Z. *Starch/Stärke* **2007**, *59*, 258.
54. Mendez-Hernandez, M. L.; Tena-Salcido, C. S.; Sanoval-Arellano, Z.; Gonzalez-Cantu, M. C.; Mondragon, M.; Rodriguez-Gonzalez, F. J. *Polym. Bull.* **2011**, *67*, 903.
55. Sharma, N.; Chang, L. P.; Chu, Y. L.; Ismail, H.; Ishiaku, U. S.; Mohd Ishak, Z. A. *Polym. Degrad. Stab.* **2001**, *71*, 381.
56. Yang, X.; Ding, X. *Geotext. Geomembr.* **2006**, *24*, 103.
57. Jordens, K.; Wilkes, G. L.; Janzen, J.; Rohlfing, D. C.; Welch, M. B. *Polymer* **2000**, *41*, 7175.